Florida Center for Advanced Aero-Propulsion (FCAAP) – *Annual Technical Symposium 2010*

Three-dimensional Modeling of Microscale Plasma Actuators

Tomas Houba, Chin-Cheng Wang, Subrata Roy

Florida Center for Advanced Aero-Propulsion (FCAAP)
Applied Physics Research Group (APRG), University of Florida, Gaineville, FL 32611
{tomash6, james614, roy}@ufl.edu

Abstract. We present a three-dimensional simulation of dielectric barrier discharge (DBD) using the finite element based multiscale ionized gas (MIG) flow code. Multispecies hydrodynamic plasma model coupled with Poisson potential equation and Navier-Stokes flow equations are solved to predict complicated flow structures inside a small channel induced by micron size actuators. Such actuators are plasma driven and have been shown to generate large electric field. Our research predicts that these actuators may potentially produce orders of magnitude higher force density than the state of the art. An experimental microactuator array is now being built under a separate AFOSR program and is ready to be tested to validate these predictions. At such small scales non-equilibrium interactions become important. Therefore, the eight-species air chemistry model is also being augmented with the Landau-Teller vibrational relaxation model through AFRL/RB collaboration to accurately capture the non-equilibrium physics of weakly ionized gas at microscale. Park's dissociation model is utilized to couple the vibration and dissociation processes for predicting the charge separation and electrodynamic force. Numerical results for the microactuator closely match reported experimental data for electric field distribution. The ion and electron density distributions are computed for an array of linear and serpentine micro actuators and the resultant electric force is employed in the flow equations. A plasma induced gas flow rate of 1.5 ml/min predicted due to such actuator arrangement in a plasma micropump.

Keywords: microscale plasma actuators, 3-D plasma gas interaction, non-equilibrium air chemistry, micropump

1 Introduction

Over the last decade, many experiments and numerical simulation show that DBD actuators produce effects on drag reduction inside the boundary layer [1]. However, these traditional macroscale DBD actuators suffer from relatively small actuation at high speed flow (> 30 m/s). As a remedy, microscale plasma actuators may induce orders of magnitude higher force density [2]. The majority of interelectrode spacing of a macroscale plasma actuator is the space charge limited quasi-neutral plasma region which does not produce any force but expends energy. The force is generated inside the space charge separated micron scale Debye sheath region. Thus the idea is to minimize the momentum and energy loss by reducing the interelectrode gap to Debye scale (a few microns). Also, thinner dielectrics generally mean lower resistance and higher capacitance. So, for a smaller gap between the electrodes, one may generate plasma at a lower voltage and with orders of magnitude lower power (milliwatts versus watts). However, plasma discharge in microactuators is quite unexplored due to limited knowledge of fundamental discharge physics at micro scale governing the interaction between charged particles, the thin insulator material(s) and the working gas. As the gap between electrodes reduces the Paschen's law dictating Townsend breakdown deviates. Also the discharge becomes unstable. Numerical investigations of such systems generally fall into three major categories: (1) hydrodynamic model, (2) kinetic model, and (3) hybrid kinetic-fluid simulation model. The hydrodynamic model holds a numerical advantage over these models in the treatment of high density plasma, where the particle approaches become prohibitively expensive. In this paper, we choose the drift-diffusion hydrodynamic model which is the most popular due to its effective capturing of the overall physics of the atmospheric plasma at a low computational cost.

Micro discharges are becoming widely popular in a variety of applications such as plasma micropump. Roy [3] presented a concept of EHD micropump using microscale plasma actuators. Such design leverage several advantages of non-mechanical micropumps. Our recent two-dimensional hydrodynamic model of microscale direct current (DC) volume discharge [2] shows very good agreement with published experimental data. The results mimic trend at both macro and microscale discharge, but the sheath structure dominated the inter-electrode region as

the gap size lessens (< 50 microns). The force density is also found to be orders of magnitude higher than the macro (mm size) plasma actuator [2]. An experimental microactuator array is now being built under a separate AFOSR program and is ready to be tested to validate these predictions [4]. However, the net force (flow) inducement remains similar to that of standard actuator due to orders of magnitude smaller plasma region than the traditional counterparts. Such two dimensional models are limited especially for a three-dimensional geometry. Thus, for a better design of the plasma micropump, it is important to identify three-dimensional effects on plasma and gas flow fields. So far, very little work has been done on plasma micropump in three-dimensional simulation.

Recent 2010 AFOSR-UFL Joint DBD Plasma Actuator Workshop [5] outlined opportunities and specific activities to advance the state of the art in plasma actuator modeling. The area of non-equilibrium physics, namely vibrational kinetics, was identified as one of the directions for pushing the boundaries of high fidelity modeling beyond the current state of the art. Vibrational plasma kinetics has been studied extensively in literature [6-7]. Models of various complexity exist that describe the highly non-equilibrium processes that occur in the discharge. These processes have been studied with the aid of the Boltzmann equation, such as to calculate the electron energy distribution function [8]. There are many phenomenological models that exist for the estimation of the rate constants and relaxation times for the non-equilibrium processes. The current model is the first effort to take into account some of these complicated processes when modeling DBD plasma actuators.

This report documents our progress in above research areas. We first predict flow inducement inside a three-dimensional DC plasma micropump using our in-house microscale ionized gas (MIG) flow code. The ion density, electron density, and electric field are solved based on first-principles. The obtained electric force density ($F = eqE$) from plasma simulation is employed as a local body force term in the Navier-Stokes equation. Then, we discuss vibrational non-equilibrium physics in plasma discharge. Park's dissociation model is utilized to couple the vibration and dissociation processes. One application of non-equilibrium air chemistry could be pyrolysis gas flow in ablative materials. We have implemented the discontinuous Galerkin (DG) methods into our already existing in-house modular MIG flow code and successfully applied it to solve 1-D thermal ablation problem using a time implicit backward Euler scheme. The main purpose of this report is to summarize the following major works: (1) Numerical simulation of fully three-dimensional plasma discharge at microscales. (2) Non-equilibrium plasma physics with air chemistry. Section 2 provides the governing equations for plasma, fluid flow, and energy as well as problem descriptions. Section 3 shows results of plasma micropumps. Conclusions are summarized in the section 4.

2 Numerical Model Descriptions

The system of nonlinear partial differential equations is solved using the finite element based MIG code. If we denote the differential equation using the linear operator $L(\cdot)$, then the system of equations can be written as $L(q)=0$ where q is the vector containing the state variables. Multiplying this equation by a permissible test function ψ and integrating over a discretized domain Ω yields the Galerkin weak statement (GWS). The discretized Galerkin weak statement is written as $WS^h = S_e\left(\int_{\Omega_e}\left[\psi L(q)\,d\tau\right]\right)_e = 0$, where S_e is a non-overlapping sum which designates the assembly of the integrals evaluated on each element Ω_e. It is given the symbol S_e to distinguish it from regular summation. The test function in the GWS is chosen orthogonal to the trial function to ensure that the error is minimum. The resulting matrix equation is solved with the nonlinear Newton-Raphson scheme using a generalized minimal residual (GMRES) solver to handle the sparseness of the stiffness matrix. The convergence criterion is based on the ℓ^2-norm of the change in the solution Δq and the residual at each time step. The convergence criterion for the problem is met when the residuals for all the conserved variables fall below 10^{-3}.

The air chemistry model that forms the starting point of the analysis is taken from Singh and Roy [9]. The air species considered in the model are N_2, N, N_2^+, O_2, O, O^-, O_2^+ and e^-. The metastable species along with N_4^+ and O_4^+ are neglected due to their high recombination rates. NO and its relevant reactions are also neglected from the

current model at this time, further simplifying the computations. The eight reactions that govern the chemistry of the discharge are taken from Ref. 9.

The original reaction rate coefficients for the chemical reactions above are given by Kossyi *et al*. [10] as functions of electron temperature. Since ion and electron temperatures vary by two orders in atmospheric DBD actuators, vibrational nonequilibrium plays an important role. Ion and electron reaction rates take into account the vibration-dissociation coupling, and are modified using a model described by Park [11]. The effective temperature of the processes involving electron impact is taken as $T_{eff} = \sqrt{T_V T_e}$. The vibration-dissociation coupling is incorporated into the model through the introduction of this effective temperature. The original reactions rates are derived using a one temperature model, so using the effective temperature introduces vibrational temperature dependence and thus accounts for the vibration-dissociation effect [11].

The present model is also being augmented with the influence of vibrational relaxation on the physics of the gas discharge. This model suitable also for high speed nonequilibria is being developed in collaboration with AFRL/RB through a separate program. Here the rotational and translational degrees of freedom are treated as if they had already attained equilibrium by the scaling argument presented in Capitelli *et al.* [12]. As the first approximation, the diatomic molecules are treated as harmonic oscillators of two vibrational levels according to the Landau-Teller theory [13]. The change in the vibrational energy due to the vibrational-translational (VT) energy exchange can be written as $\dot{e}_{VT} = \dfrac{e_V^* - e_V}{\tau_r}$. The vibrational temperature can be calculated from the vibrational energy by inverting the harmonic oscillator relation $e_V = \dfrac{R\Theta_V}{\exp\left(\Theta_V / T_V\right) - 1}$. The vibrational energy at equilibrium e_V^* can be obtained by simply substituting the translational temperature T in place of T_V, since they are identical at thermal equilibrium. Θ_V is the species characteristic vibrational temperature and R is the gas constant. The relaxation time τ_r is modeled based on expressions from Millikan and White [14]. Neglecting thermal conduction effects and other vibrational energy exchange mechanisms, the vibrational energy conservation equation can be written as $\dfrac{\partial\left(n_\alpha e_{V\alpha}\right)}{\partial t} + \nabla\cdot\left(n_\alpha \mathbf{v}_\alpha e_{V\alpha}\right) = n_\alpha \dot{e}_{VT} + \dot{\omega}_\alpha e_{V\alpha}$. The vibrational energy equation is solved for each of the diatomic species N_2, N_2^+, O_2 and O_2^+. The source term $\dot{\omega}_\alpha$ represents the change in chemical composition of species α. The electron temperature is obtained by first solving the electron energy conservation equation. $\dfrac{\partial}{\partial t}\left(n_{e^-} e_{e^-}\right) + \nabla\cdot\left(n_{e^-}\mathbf{v}_{e^-} e_{e^-}\right) = \boldsymbol{j}_{e^-}\cdot\boldsymbol{E} + \dot{\omega}_{e^-} e_{e^-} + \dot{Q}_{coll}$. The electron temperature can be calculated from the electron energy based on the electron specific heat. The ideal gas law $p = nk_B T$ is used to close the equation system.

3 Results and Discussion

3.1 Benchmarking of Actuator Model

We first benchmark our numerical prediction for a macroscale dielectric barrier discharge (DBD) actuator laid on a flat plate in Figure 1a. A potential difference of 16 kV_{pp} is applied to the powered electrode. The induced flow is simulated under quiescent condition using the air chemistry based reduced order plasma formulation [15]. The numerically predicted streamwise velocity of the induced flow compares very well with experimental data [16] collected for the same actuator with the same electrical and geometric parameters. We also compare our numerical results for microscale discharge with experimental data reported in the literature. Figure 1b shows excellent agreement between experimental electric field data from Longwitz [17] with that predicted by MIG using first principles based gas discharge simulation as the interelectrode gap reduces from 50 to 5 μm. The computed charge density slightly decreased as the gap g decreased, but it increased at the gap below 10 μm because much less electrons exist in the plasma region. Based on the calculation of the electric force (qE), we can see the force F_y is 1 MN/m^3 at 20 micron gap. Note that such force density is three orders of magnitude higher than that of macro

plasma actuators. As the gap decreases force seem to increase exponentially. For example, at five micron gap the force density increases approximately seven fold to 6.8 MN/m^3. This physics of such high thrust generation remains to be characterized and validated experimentally.

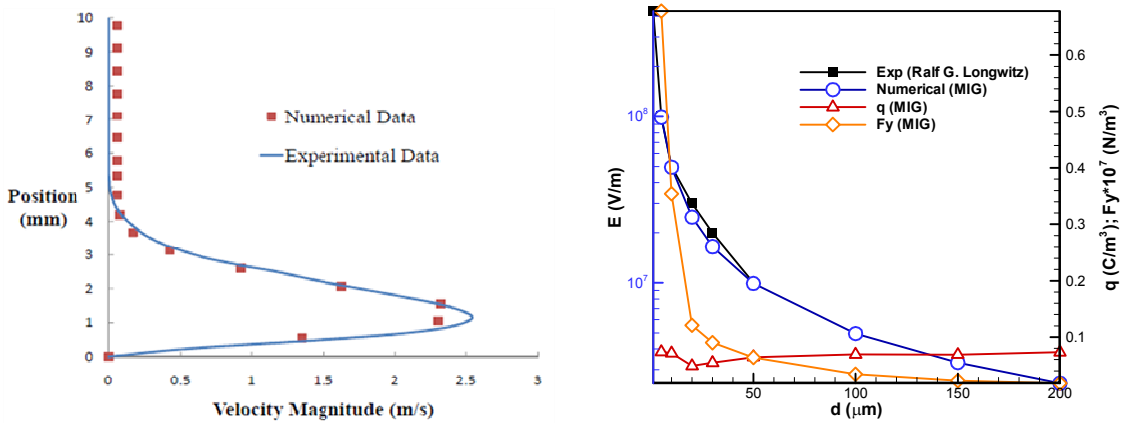

(a) Macroscale actuator at 16 kV_{DD} (b) Microscale actuator

Fig. 1. Comparison of numerical result with experimental data.

3.2 Three-dimensional Micropump Simulation

Figure 2 shows a schematic of plasma micropump of isometric view. The tri-directional pump draws the fluid into the channel at inlets due to the attraction of parallel plasma actuators and drains the fluid upward to the outlet by means of horseshoe plasma actuators. The horseshoe actuator consists of semi-circle and parallel electrodes. For less computational costs, we neglect the thickness of the electrodes and simulate a half of the plasma micropump due to the symmetric configuration.

The computational mesh for this domain size consists of (48x48x41) 276,480 elements and 289,933 nodes. The mesh density is on the order of Debye length which is sufficient to capture the physics of plasma dynamics. The powered electrodes (red), grounded electrodes (black) and dielectric (grey) are shown in figure 2. For the plasma boundary conditions, DC potential is applied to powered electrode of $\phi = 80$V (with corresponding nominal electric field of 30 kV/cm). All plasma and gas properties are based on 5 torr pressure. The inlets and outlet flow boundary conditions are employed zero gauge pressure and dielectric surface is assumed no-slip wall condition. We assume symmetric boundary condition at the center of the plasma micropump. In microscale flows, Knudsen number (Kn) is an important dimensionless parameter that determines the validity of continuum model for different regimes of fluid flow [18]. The Knudsen number is defined as the ratio of the fluid mean free path λ and macroscopic characteristic length Λ, i.e. Kn = λ/Λ. For the flow problem, the Kn is less than 10^{-2} assuring continuum flow with no-slip wall boundary condition. Due to several orders of magnitude difference in timescales of plasma and gas flow, we employ the time average of electric body force $F_j = eqE_j$ in the Navier-Stokes equations. Figure 3a shows the charge separation overlaid with force vectors at $y = 0.3$. The peak of charge separation ($q = n_i - n_e$) is close to the powered

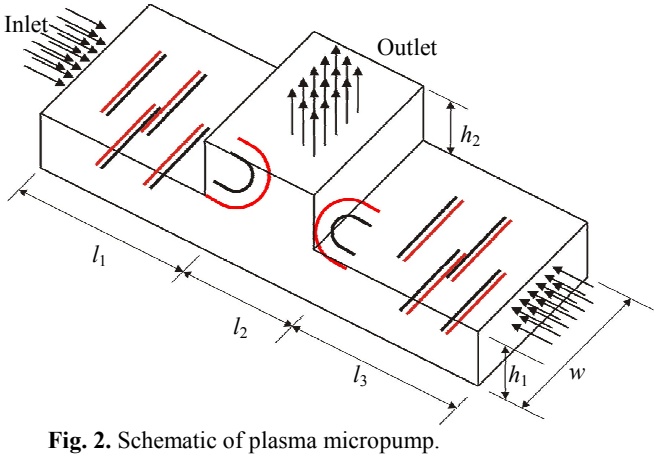

Fig. 2. Schematic of plasma micropump.

electrode. The strongest force vectors is also close to the powered electrode because the time average of electrostatic force per volume ($F = eqE$) is function of charge separation and electric field.

We also can see that the force vectors are acting from the powered electrode to the grounded electrode following electric field lines. Potential distribution is solved by Poisson equation and matches the boundary condition from 80V to 0V. The electric force density is applied to the flow field to actuate the fluid flow shown in figure 3b. The electric force draws the fluid from the left inlet and drains the fluid upward to the top outlet. The contour is colored by z-component velocity and shows the highest upward velocity close to the corner of the plasma micropump.

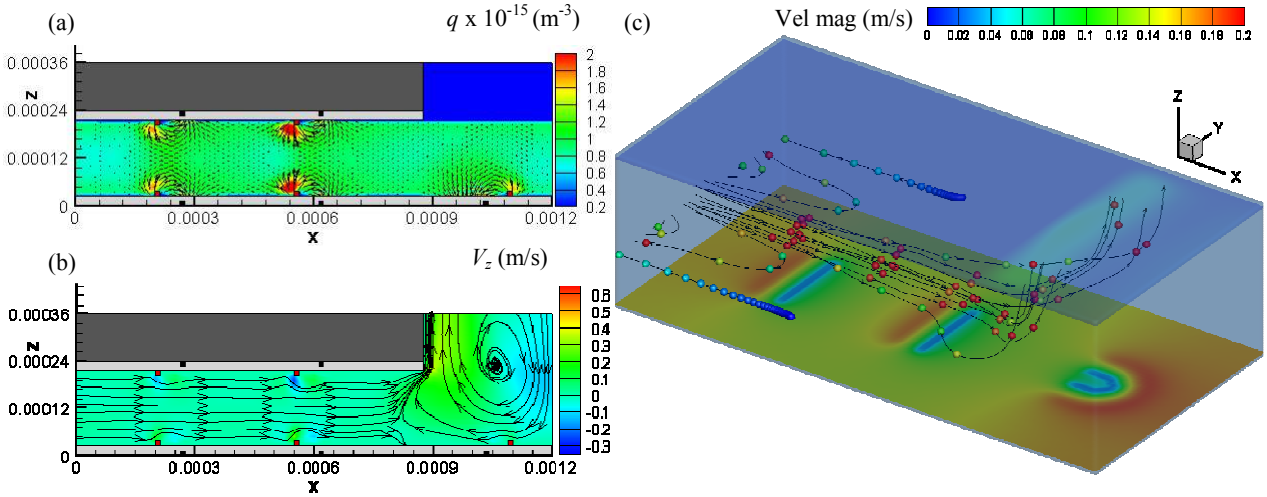

Fig. 3. (a) Charge separation (q) overlaid with force vectors at xz-plane. (b) Velocity contour (V_z) overlaid with streamtraces at xz-plane (y = 0.3 mm). **(c)** Fluid particles overlaid with velocity magnitude (top wall) and potential (bottom wall).

Evidently, the horseshoe plasma actuator is inducing a flow tripping mechanism that produced vortical structures at the symmetric plane (right). Such vortical structures were not found in previous two-dimensional simulation. Figure 3c shows fluid particles are colored by velocity magnitude in isometric view. The top wall is colored by velocity magnitude, while the bottom wall is colored by potential. Based on the color of particles, fluid is moving much faster at center of the pump. Also, the streamtraces of fluid flow are much smoother. The average flow rate Q of 1.5 ml/min is calculated. This is an order of magnitude lower flow rate at 5 torr than that predicted earlier [2] at atmospheric condition.

4. Conclusions and Future Work

Plasma actuators have become an exciting research topic due to their possible usefulness in a wide range of applications. One of the best ways to simulate the plasma discharges occurring in these devices is to use a fluid dynamics approach which is derived from the conservation equations and couple it with Maxwell's equations, notably the Poisson equation. The present model is based on a high-fidelity finite-element approach embedded into the MIG flow code. We have studied realistic applications of DBD actuators in microscale using three-dimensional hydrodynamic drift-diffusion plasma model coupled with Possion equation. Numerical results predict that the microscale actuators may produce orders of magnitude higher electric force density than the macroscale actuators. An experimental microactuator array is now ready to be tested to validate these predictions under a separate AFOSR program. The vibrational relaxation model has also been identified as a first approximation to model vibrational kinetics in plasma actuators. The drift-diffusion plasma species and Navier-Stokes flow equations are solved using MIG flow code. The results show the highest charge separation and force close to the powered electrodes. We find vortical structures inside the micropump which were missing in our two-dimensional simulation. We predict an order of magnitude lower flow rate at 5 torr than that predicted earlier for atmospheric condition. However, such flow rates may be quite useful for a range of practical applications. The scope for future work includes extending

the current results to include the vibrational relaxation model. Future models should also include additional species such as O_2^- and NO, which could have a significant effect on the air chemistry. Furthermore, vibrational-vibrational and vibrational-electronic energy exchanges along with photoionization effects, which are currently neglected, may be added in future iterations of the model. All of these additions are intended to push the boundaries of the continuum approach, which is an essential endeavor if the full physics of plasma actuators are to be captured.

5. Acknowledgments

This work was partially supported by the Florida Center for Advanced Aero-Propulsion (FCAAP). Additional support came from AFOSR and Surfplasma through a grant from AFRL.

References

[1] Roy, S., Gaintonde, D., "Force Interaction of High Pressure Glow Discharge with Fluid Flow for Active Separation Control," Physics of Plasmas, vol. 13, no. 2, (2006) 023503

[2] Wang, C.C., Roy, S., "Microscale Plasma Actuators for Improved Thrust Density," Journal of Applied Physics, vol. 106, (2009) 013310.

[3] Roy, S, "Method and apparatus for efficient micropumping," PCT International Publication WO 2009/015371, International Publication date January 29, 2009.

[4] Zito, J., Arnold, D. P., "Fabrication and Electrical Characterization of Microscale Dielectric Barrier Discharge Devices," Hilton Head, June 2010.

[5] AFOSR-UFL Joint DBD Plasma Actuator Workshop, February 24-25 2010, http://cpdlt.mae.ufl.edu /DBD3Workshop/.

[6] Capitelli, M., Ferreira, C.M., Gordiets, B.F., Osipov, A.I., "Plasma Kinetics in Atmospheric Gases," Springer-Verlag, New York, 2000, Chaps. 2, 3, 13.

[7] Gordiets, B.F., Osipov, A.I., Shelepin, L.A., "Kinetic Processes in Gases and Molecular Lasers," Gordon and Breach, New York, 1988.

[8] Megill, L., Cahn, J., "The Calculation of Electron Energy Distribution Functions in the Ionosphere," J. Geophys. Res., 69(23), 1964, pp. 5041-5048.

[9] Singh, K.P., Roy, S., "Modeling plasma actuators with air chemistry for effective flow control," Journal of Applied Physics, 101 (12) 123308, 2007.

[10] Kossyi, I.A., Kostinsky, A.Y., Matveyev, A.A., Silakov, V.P., "Kinetic Scheme of the Non-equilibrium Discharge in Nitrogen-oxygen Mixtures," Plasma Sources Science and Technology, vol. 1, (1992) 207-220

[11] Park, C., "Assessment of Two-Temperature Kinetic Model for Ionizing Air," AIAA Paper 87-1574, 1987.

[12] Capitelli, M., Ferreira, C.M., Gordiets, B.F., Osipov, A.I., *Plasma Kinetics in Atmospheric Gases*, Springer-Verlag, New York, 2000, Chaps. 2, 3, 13. Josyula, E., Bailey, W., "Governing Equations for Weakly Ionized Plasma Flowfields of Aerospace Vehicles", *Journal of Spacecraft and Rockets*, Vol. 40, No. 6, 2003.

[13] Landau, L., Teller, E., "Zur Theorie der Schalldispersion," *Physikalische Zeitschrift der Sowjetunion*, Vol. 10, No. 1, 1936, pp. 34–43.

[14] Millikan, R. and White, D., "Systematics of Vibrational Relaxation," *Journal of Chemical Physics*, Vol. 39, No. 12, 1963, pp. 3209–3213.

[15] Singh, K.P., Roy, S., "Force approximation for a plasma actuator operating in atmospheric air," Journal of Applied Physics, 103 (1) 013305, 2008.

[16] Durscher, R., Cattafesta, L. and Roy, S., "Comparison of Force Measurement Techniques for a DBD Plasma Actuator," Aerospace Sciences Meeting, Orlando, 2011 (submitted).

[17] Longwitz, R.G., "Study of Gas Ionization in a Glow Discharge and Development of a Micro Gas Ionizer for Gas Detection and Analysis," PhD thesis, Institute of Microsystems and Microelectronics, Swiss Federal Institute of Technology, Lausanne, Switzerland (2004).

[18] Roy, S., Raju, R., Chuang, H.F., Cruden, B.A., Meyyappan, M., "Modeling Gas Flow Through Microchannels and Nanopores," Journal of Applied Physics, vol. 93, no. 8, (2003) 4870-4879.